第 34 卷第 4 期
2018 年 4 月

无 机 化 学 学 报
CHINESE JOURNAL OF INORGANIC CHEMISTRY

Vol.34 No.4
777-783

Pd-Ag 合金纳米线的可见光辅助简易合成及其对乙醇的电催化氧化

谭德新* 王艳丽*
(岭南师范学院化学化工学院,湛江 524048)

摘要:以硝酸钯和硝酸银为金属前驱体,乙醇和柠檬酸钠作为还原剂,聚乙烯吡咯烷酮作为稳定剂和导向剂,以普通市售白炽灯作为光源,采用简易可见光辅助液相法合成了 Pd-Ag 合金纳米线。通过 FESEM、TEM、HRTEM、PXRD 和 UV-Vis 等技术对样品的形貌、晶体结构和光学性质进行了表征,并通过循环伏安法和计时电流法研究了 Pd-Ag 合金纳米线修饰玻碳电极对乙醇的电催化氧化。与相同条件下制备的纳米钯材料相比,Pd-Ag 合金纳米线具有更好的电催化活性、抗中毒性和稳定性。

关键词:Pd-Ag 合金;纳米线;可见光;乙醇;电催化
中图分类号:O614 **文献标识码**:A **文章编号**:1001-4861(2018)04-0777-07
DOI:10.11862/CJIC.2018.098

Pd-Ag Alloy Nanowires: Facile Visible-Light-Assisted Synthesis and Electrocatalytic Activity toward Ethanol Oxidation

TAN De-Xin* WANG Yan-Li*
(*School of Chemistry and Chemical Engineering, Lingnan Normal University, Zhanjiang, Guangdong* 524048, *China*)

Abstract: Using palladium nitrate and silver nitrate as the metal precursor, ethanol and sodium citrate tribasic dehydrate as reducing agents and poly (vinyl pyrrolidone) (PVP) as a stabilizer and guiding agent, Pd-Ag alloy nanowires were synthesized via visible-light-assisted solution approach with a commercial incandescent lamp as light source. The morphologies, crystal structure and optical properties were characterized by field emission scanning electron microscopy (FESEM), transmission electron microscopy (TEM), high resolution transmission electron microscopy (HRTEM), power X-ray diffraction (PXRD), and UV-visible spectroscopy, respectively. The electrocatalytic properties of the Pd-Ag alloy nanowires modified glassy carbon electrode for ethanol oxidation were investigated by cyclic voltammetry and chronoamperometry. The Pd-Ag alloy nanowires exhibited much better electrocatalytic performance than Pd nanoparticles toward ethanol oxidation reaction in alkaline media in terms of the electrocatalytic activity, anti-poisoning ability and stability.

Keywords: Pd-Ag alloy; nanowires; visible light; ethanol; electrocatalysis

0 Introduction

Direct liquid fuel cells, especially direct ethanol fuel cells (DEFCs), is considered to be one of the promising clean energy sources with high energy conversion efficiency and low environmental pollution[1-2]. Up to now, designing highly efficient catalysts is still the main challenges for DEFCs applications. Pd-based catalysts, because of their low cost and good tolerance to the poisoning caused by intermediate species

收稿日期:2017-11-09。收修改稿日期:2018-01-22。
国家自然科学基金(No.51303005)、广东省科技发展专项资金项目(No.2017A030307028)、扬帆计划引进紧缺拔尖人才项目(No.0003017011)和岭南师范学院校级科研项目(No.1170917014)。
*通信联系人。E-mail:ylwang1998@163.com,tdxin@163.com

during the ethanol oxidation process, are likely to be put into practical use for DEFCs[3]. Particularly, the incorporation of a second metal (M) into Pd for forming PdM alloy often brings superior catalytic performance, due to the synergistic effects and rich diversity of the compositions[4]. Recently, several PdM catalysts, such as Pd-Ag[3], Pd-Cu[5] and Pd-Sn[6], demonstrate the enhanced catalytic activity toward the ethanol oxidation reaction (EOR). For example, well-dispersed *fcc*-Pd-Cu alloys are successfully prepared by one-pot synthesis and a two-step reductive process, and show an excellent catalytic activity, durability and catalytic stability toward EOR[5]. On the other hand, specific structures, such as one-dimensional (1D) bimetallic nanowires or nanotubes[7], threedimensional (3D) noble metal networks (NWs)[3], nanoflowers[8], nanoneedles[9], or core-shells[10], have significant effects on the properties of the materials. Among them, 1D bimetallic nanowires exhibit enhanced electrocatalytic activity for fuels anodic oxidation and oxygen cathodic reduction owing to the large specific interface areas. Recently, Chen et al.[2] synthesized bimetallic Pd-Ag alloy nanowires at 170 ℃ with oil bath by one-step wet chemical strategy, exhibiting enhanced catalytic activity for formic acid oxidation. Compared to the conventional heat treatment methods, the products are more uniform and the growth mechanism can be more conveniently resolved using photochemical and irradiation synthesis methods[11-13]. These simple processes have proven to be a promising route for the preparation of Pd-based catalysts. Current photochemical methods focus mainly on the use of high-energy radiation, such as UV light or γ-irradiation. For instance, Nenoff et al.[14] have successfully prepared Ag-Ni alloy nanoparticles and Pd-Ni alloy nanoparticles via a ^{60}Co-γ source. Pande et al.[15] have reported the synthesis of monometallic (Au and Pd) and bimetallic (AuPd) nanoparticles using graphitic carbon nitride quantum dots under the UV lamp (λ=365 nm). Therefore, it is important to design a safer, cheaper, and more facile light-assisted method to synthesize 1D Pd-based alloy nanostructures. Recently, we have presented a novel visible-light-assisted method to synthesize Pd nanoparticles with single-crystalline and multiple-twinned structures[16-17]. However, to the best of our knowledge, there have been few reports on visible light-assisted synthesis of Pd-based alloy, especially with 1D nanowires structures. Thus, we have geared our efforts towards exploring a simple, inexpensive, and efficient approach to the large-scale fabrication of 1D Pd-based alloy nanostructures.

In this paper, a facile and environmentally friendly visible-light-assisted method has been developed for the synthesis of 1D Pd-Ag alloy nanowires under the irradiation of visible light from a commercial incandescent lamp. The unique nanowires were produced by the coreduction of Pd and Ag precursors in the presence of sodium citrate tribasic dehydrate and poly (vinyl pyrrolidone). The as-prepared Pd-Ag nanowires exhibited excellent electrocatalytic activity toward EOR.

1 Experimental

1.1 Chemicals and materials

Palladium nitrate ($Pd(NO_3)_2\cdot 2H_2O$, >99.9%), silver nitrate ($AgNO_3$, >99.8%) and poly (vinyl pyrrolidone) (PVP, M_W=58 000) were purchased from Sinopharm Chemical Reagent Co., Ltd. Sodium citrate tribasic dehydrate ($Na_3C_6H_5O_7\cdot 2H_2O$, >99%) and ethanol were obtained from Nanjing Chemical Reagent No.1 Factory. All other chemicals were analysis reagent (AR) grade and used as received.

1.2 Synthesis of Pd-Ag alloy nanowires

In a typical synthesis, sodium citrate tribasic dehydrate (3.4 mmol), PVP (1.7 mmol), $Pd(NO_3)_2\cdot 2H_2O$ (26.27 mmol) and $AgNO_3$ (30.61 mmol) was mixed with 20 mL of ethanol and 4 mL of deionized water in a glass vessel. The mixture was dispersed to form a homogeneous solution by constant strong stirring for 10 min at room temperature. Then, the mixture was irradiated under constant stirring for 2 h with visible light from the 200-Watt incandescent lamp at a distance of 5 cm (5.30 mW·cm^2 put on the reacting mixture). Two hours later, the temperature of mixture was 78 ℃. The color of solution was gradually changed from pale yellow to dark. The dark suspensions were

precipitated by acetone and washed at least three times with ethanol to remove excess metal precursors and PVP. The final dark product could be easily redispersed in ethanol solvents to yield a clear homogeneous solution. As a comparison, Pd and Ag nanomaterials were synthesized using the same method. The final products were denoted as Pd, Ag and Pd-Ag, respectively, according to the different compositions.

1.3 Characterization

Transmission electron microscopy (TEM) images, high resolution transmission electron microscopy (HRTEM) images, selected area electron diffraction (SAED) patterns and energy dispersive spectrometer (EDS) were carried out on a JEM-2010 instrument operated at 200 kV. Field emission scanning electron microscopy (FESEM) images were performed with a Sirion 200 instrument. Powder X-ray diffraction (PXRD) pattern was recorded on a XD-3 type X-ray diffractometer employing Cu $K\alpha$ radiation (λ=0.154 06 nm) for scattering angles $25° \leqslant 2\theta \leqslant 90°$ with 36 kV and 30 mA. UV-visible spectroscopy of the prepared suspensions was obtained by an UV-visible spectrophotometer (UV-2600) from Shimadzu with quartz cuvettes. The intensity of the light was detected by a FZ400 visible light power meter.

1.4 Electrochemistry tests

Electrochemical measurements were performed with a CHI 660E electrochemical workstation (CH Instruments, Chenhua Co., Shanghai, China) at room temperature, and conducted on a conventional three-electrode cell, which includes a platinum wire as counter electrode, a saturated calomel electrode (SCE) as reference electrode and the nanomaterials-modified glassy carbon electrode (GCE, 3 mm in diameter) as working electrode. In all electrochemical measurements, the current densities were normalized to the geometric surface area of the GCE.

For the preparation of the nanomaterials modified electrode, 6 μL of a suspension containing nanomaterials (nanomaterials concentration=1 $g \cdot L^{-1}$) was dropped on the clean electrode surface (the area of the electrode=7.065×10^{-2} cm^2) and dried in air. Next, the Nafion film was prepared by dropping 3 μL of a Nafion solution (0.1%, *w*/*w*) onto the electrode and allowed the solvent to evaporate at room temperature. The solutions were deaerated thoroughly for at least 30 min with pure nitrogen gas and kept under a positive pressure of this gas during the experiments. All experiments were performed at room temperature.

2 Results and discussion

2.1 Characterization of Pd-Ag alloy nanowires

The crystalline phase of the Pd-Ag alloy nanowires was further studied with PXRD measurement as shown in Fig.1. For comparison, the PXRD patterns of Pd and Ag are also displayed in Fig.1. In the pattern of Pd, the peaks at ca.40.01°, 46.52°, 68.11°, 82.00° and 86.40° represent the Pd (111), Pd (200), Pd (220), Pd (311) and Pd (222) planes, respectively. Compared to the data of Pd, the diffraction peaks from Pd-Ag nanowires shift to lower 2θ values, suggesting the reduction in lattice constant. Here, all the diffraction peaks from Pd-Ag nanowires locate between the positions expected for the Pd and Ag, indicating the obvious alloying of Pd and Ag. Such PXRD phenomenon has also been observed with other bimetallic alloy nanostructures[2-3]. Moreover, neither a Pd nor an Ag single component peak was detected, confirming the presence of only single-phase Pd-Ag alloys. It also should be noted that, from the PXRD pattern of Pd-Ag, the intensity ratio between the diffraction peaks of Pd (111) and Pd (200) is 2.13, suggesting the abundant (111) planes of the Pd-Ag

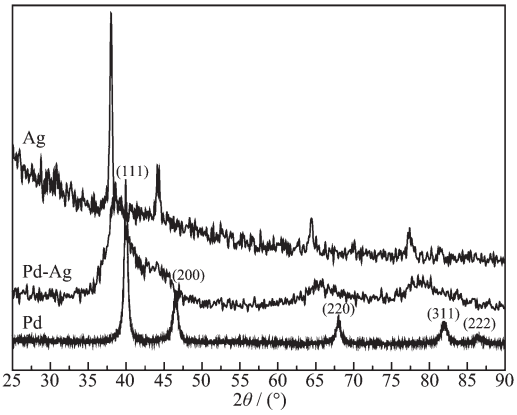

Fig.1　PXRD patterns of Pd, Ag and Pd-Ag alloy nanowires

nanowires. The bimetallic Pd-Ag nanoparticles′ size can be calculated according to Scherrer equation[18]:

$$L=\frac{0.9\lambda_{K\alpha_1}}{B_{2\theta}\cos\theta_{\max}}$$

where L is the size of Pd-Ag nanoparticles. $\lambda_{K\alpha_1}$ is the X-ray wavelength (λ=0.154 nm). $B_{2\theta}$ is the half-peak width. $\theta_{\max}$ is the Bragg angle. The calculated nanoparticle size of Pd-Ag nanowires is 4.89 nm, which agree with the TEM results very well.

The morphologies of the as-synthesized materials were characterized by FESEM (Fig.2(A)) and TEM (Fig.2(B,C)) measurements, which confirms the formation of the nanowires by a facile visible-light-assisted method. It can be seen that, uniform nanowires with high yield were obtained. The length of such nanowires can reach up to 250 nm with average diameters of 4 nm. For a single nanowire, it consists of interconnected nanoparticles (top left inset in Fig.2 (C)). To investigate the crystal structures of the synthesized Pd-Ag nanowires, HRTEM analyses were also performed (Fig.2(D)). Well-resolved lattice fringes can be seen in Fig.2(D). PXRD result is consistent with (111) interplanar spacing found in the HRTEM measurements. By careful measurements, it was found that there is mainly one type of lattice fringes with interplanar spacing of 0.23 nm, which is ascribed to the (111) lattice plane of the Pd-Ag alloy nanostructure. The lattice fringes are not continuous and their orientations vary, demonstrating that the interconnected Pd-Ag nanowires are polycrystalline. This is further confirmed by the selected area electron diffraction (SAED) pattern, as shown in Fig.2(B), inset. The morphology of such ultrathin nanowires is very similar to that of other two-step synthesized Pd-Pt[19] and one-step synthesized Pd-Ag nanowires at 170 ℃ with polyol reduction method[2]. So the present report provides a facile route for preparing bimetallic alloy nanowires. From EDS analysis shown in Fig.2(E), both Pd and Ag are present in the nanowire materials in addition to the Cu substrate. The average molar ratio of Pd to Ag is determined to be 46∶54 based on the EDX measurement, which is close to 26.27∶30.61. It is clear that the precursors can be largely reduced in the presence of sodium citrate tribasic dehydrate and ethanol[3].

Fig.3 shows the UV-Vis absorption spectra of Ag, Pd-Ag and Pd nanoparticles in colloid state. In Fig.3, a distinct band is observed at 411 nm for Ag colloid that must be due to the localized surface plasmon resonance (SPR) excitation of the Ag nanoparticles[20].

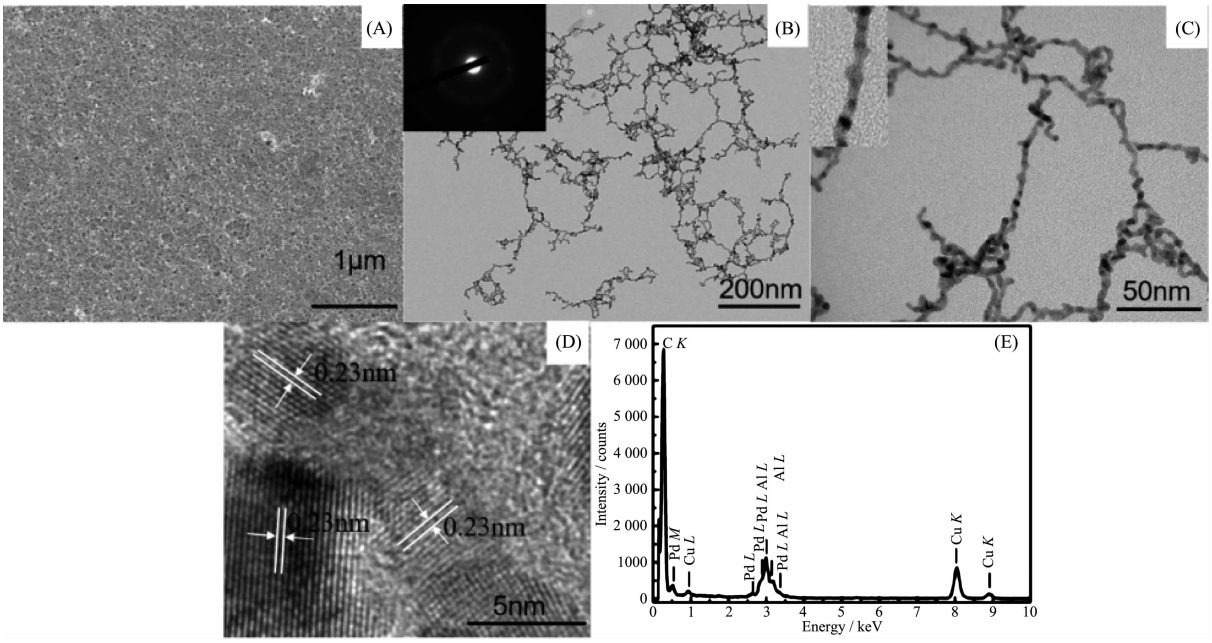

Fig.2 (A) FESEM image, (B) TEM image and the corresponding SAED pattern (inset), (C) high-magnification TEM image, (D) HRTEM image, and (E) EDX spectrum of Pd-Ag alloy nanowires

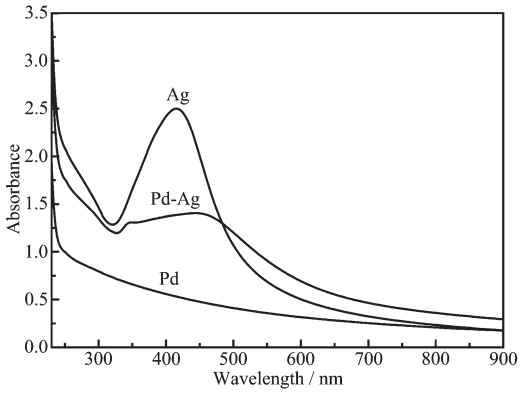

Fig.3　UV-visible spectroscopy of Pd, Ag and Pd-Ag alloy nanowires

It is noteworthy that this band is gradually weakened, with a clear red-shift, as Pd is added to form Pd-Ag alloy, and no UV-Vis absorption is seen at all for pure Pd colloid. The UV-Vis absorption characteristics here also agree well with the Pd-Ag alloy reported previously, indicating Pd-Ag nanoparticles are present in a form of homogeneous alloy[20-21].

2.2　Ethanol oxidation with Pd-Ag alloy nanowires

The electrocatalytic activities of Pd nanoparticles and Pd-Ag nanowires were studied by cyclic voltammetry (CV) from −0.8 to 0.3 V with the same Pd loading. Fig.4(A) shows the typical CV curves of Pd and Pd-Ag nanowires in N_2-saturated 1 mol·L^{-1} KOH solution. Both samples present reduction peaks of palladium oxides between −0.60 and −0.20 V in the negative scan. Pd-Ag alloy present the highest reduction peak. In the positive scan, OH^- was adsorbed onto the surface of catalysts. In comparison with Pd nanoparticles, Pd-Ag alloy shows a more negative onset potential, indicating the easier adsorption of OH^- on the surface[3].

According to the CV curves in Fig.4(A), the corresponding ECSA of each catalyst was calculated by quantification of the electric charges associated with the reduction of PdO[22], as shown in the following equation[4]:

$$\mathrm{ECSA}=\frac{Q}{mCv}$$

where Q is the charge for PdO reduction on the surface, which can be obtained from the area integral of Fig.4(A). m is the mass of Pd (6 μg). C is the charge required to reduce the layer of PdO (420 μC·cm^{-2}). v is the scan rate, which is 50 mV·s^{-1}. The calculated ECSA is listed in Table 1. It has been demonstrated that ECSA dominates the electrocatalytic activity of catalyst materials. Higher ECSA contributes to an increase of ethanol oxidation reaction activity and thus an increase of the overall fuel cell performance[23]. The specific ECSA of the Pd-Ag alloy nanowires (71.43 $m^2 \cdot g_{Pd}^{-1}$) is higher than the Pd nanoparticles (37.57 $m^2 \cdot g_{Pd}^{-1}$).

Fig.4(B) shows the second voltammogram run with Pd nanoparticles and Pd-Ag nanowires modified electrode in 1 mol·L^{-1} KOH containing 1 mol·L^{-1} ethanol, respectively. Both samples display a typical current peak in the forward scan, representing the oxidation of ethanol. The onset potential and peak current of Pd and Pd-Ag catalysts are summarized in Table 1. A more negative onset potential and higher

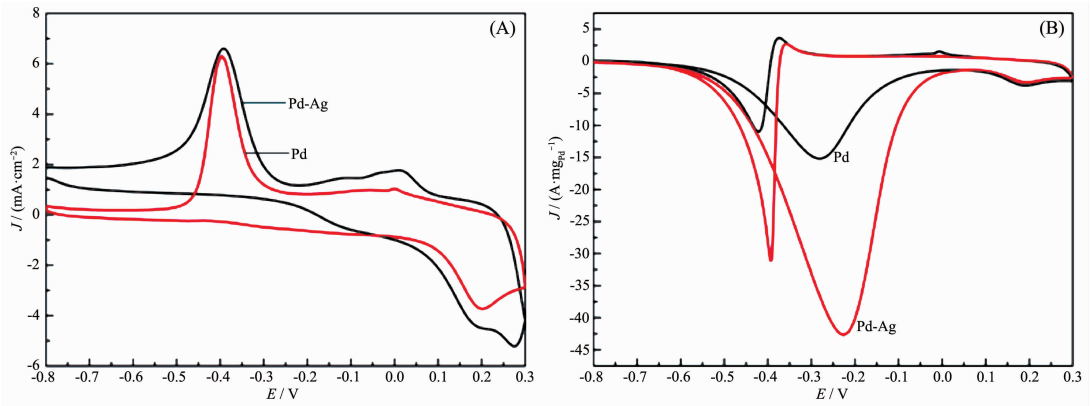

Fig.4　CV curves of Pd and Pd-Ag catalysts in N_2-saturated 1 mol·L^{-1} KOH (A) and 1 mol·L^{-1} KOH+1 mol·L^{-1} CH_3CH_2OH solution (B) at a scan rate of 50 mV·s^{-1}

Table 1 Electrochemical parameters of Pd and Pd-Ag alloy nanowires

Material	Onset potential / V	Peak current / ($A \cdot mg_{Pd}^{-1}$)	I_f/I_b	ECSA / ($m^2 \cdot g_{Pd}^{-1}$)
Pd	−0.56	15.42	1.26	37.57
Pd-Ag	−0.66	42.93	1.43	71.43

peak current were presented on Pd-Ag alloy nanowires compared to Pd nanoparticles. In the backward scan, another oxidation peak is formed on the two CV curves, which is associated with the oxidation of intermediates of ethanol dissociative adsorption. The accumulation of these intermediates will cause "catalyst poisoning" [24-25]. The ratio of forward peak current density (I_f) to backward peak current density (I_b) is used to evaluate the catalyst tolerance to carbonaceous intermediates accumulation[26]. The ethanol oxidation reaction test results show that the I_f/I_b values of the synthesized Pd-Ag alloy nanowires are larger than that of Pd, indicating the better tolerance to carbonaceous intermediates accumulation of as-prepared nanowires.

The CV curves of the ethanol oxidation reaction on the Pd-Ag alloy nanowires catalyst in 1.0 $mol \cdot L^{-1}$ KOH containing 1.0 $mol \cdot L^{-1}$ ethanol at different scan rates is shown in Fig.5(A), and the insert shows the relationship between the peak current density and the square root of scan rate. As can be seen, the peak current densities are linearly proportional to the square root of the scan rates, suggesting that the ethanol oxidation reaction on the Pd-Ag nanowires catalyst in alkaline media may be controlled by a diffusion process[27-28].

To investigate the electrocatalyst stability of Pd nanoparticles and Pd-Ag alloy nanowires, chronoamperometric tests were carried out on the catalysts at a potential of −0.3 V for 2 000 s in N_2-saturated 1 $mol \cdot L^{-1}$ KOH +1 $mol \cdot L^{-1}$ CH_3CH_2OH solution, as shown in Fig.5(B). Both the catalysts show a significant decay at the very beginning and then remain stable. The current decay of the EOR implies the formation of carbonaceous intermediates, which can poison the active sites of the catalysts. As expected, the Pd-Ag alloy nanowires show higher current density at the start and the end of the tests than Pd nanoparticles, indicating its better catalytic activity and stability against the poisoning[25,29].

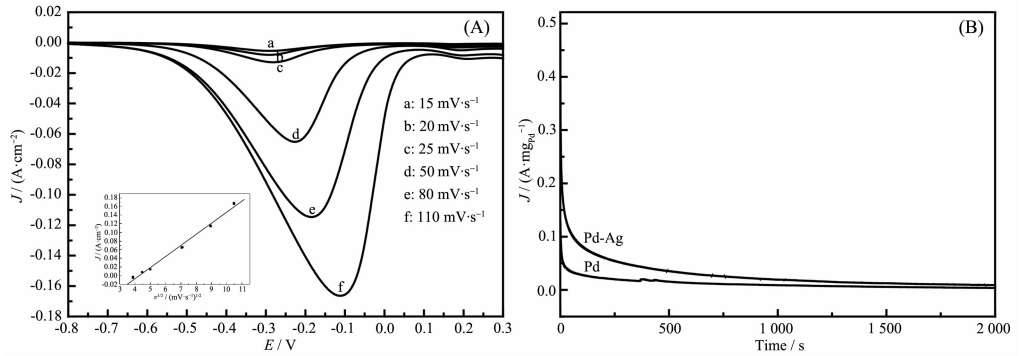

In N_2-saturated 1 $mol \cdot L^{-1}$ KOH+1 $mol \cdot L^{-1}$ CH_3CH_2OH solution

Fig.5 (A) CV curves of the Pd-Ag alloy nanowires with the various scan rates, and the insert is the dependence of cathodic peak current density on the square root of scan rate; (B) Chronoamperometric curves of Pd and Pd-Ag alloy nanowires at an electrode potential of −0.3 V

3 Conclusions

In summary, we have synthesized Pd-Ag alloy nanowires via a facile visible-light-assisted method. In cyclic voltammetric and chronoamperometric tests of ethanol oxidation, Pd-Ag alloy nanowires present much better catalytic activity with larger oxidation current density, higher ECSA, more negative onset potential, and better stability in comparsion with Pd nanoparticles. Overall, the present study not only

provides a facile one-step method to prepare alloy nanowires, but also find the obtained Pd-Ag electrocatalyst with high catalytic performance for application in fuel cells.

References:

[1] Puthiyapura V K, Brett D J L, Russell A E, et al. *ACS Appl. Mater. Interfaces*, **2016**,**8**(20):12859-12870

[2] Lu Y Z, Chen W. *ACS Catal.*, **2012**,**2**(1):84-90

[3] Fu S F, Zhu C Z, Du D, et al. *ACS Appl. Mater. Interfaces*, **2015**,**7**(25):13842-13848

[4] Zhang Q L, Feng J X, Wang A J, et al. *RSC Adv.*, **2014**,**4**(95):52640-52646

[5] Xue J, Han G, Ye W, et al. *ACS Appl. Mater. Interfaces*, **2016**,**8**(50):34497-34505

[6] Du W X, Mackenzie K E, Milano D F, et al. *ACS Catal.*, **2012**,**2**(2):287-297

[7] Nasrollahzadeh M, Azarian A, Ehsani A, et al. *Tetrahedron Lett.*, **2014**,**55**(17):2813-2817

[8] Ahmed M S, Jeon S. *J. Electrochem. Soc.*, **2014**,**161**(12):F1300-F1306

[9] Lu Y Z, Chen W. *J. Phys. Chem. C*, **2010**,**114**(49):21190-21200

[10]Jiang Y Y, Lu Y Z, Han D X, et al. *Nanotechnology*, **2012**, **23**(10):105609-105617

[11]Zhang B, Dai W, Ye X C, et al. *Angew. Chem. Int. Ed.*, **2006**,**45**(16):2571-2574

[12]Kim F, Song J H, Yang P D. *J. Am. Chem. Soc.*, **2002**,**124**(48):14316-14317

[13]Xie Y, Qiao Z, Chen M, et al. *Adv. Mater.*, **1999**,**11**(18):1512-1515

[14]Zhang Z Y, Nenoff T M, Leung K, et al. *J. Phys. Chem. C*, **2010**,**114**(34):14309-14318

[15]Fageria P, Uppala S, Nazir R, et al. *Langmuir*, **2016**,**32**(39):10054-10064

[16]Tan D X, Wang Y L, Gan Y. *Rare Met. Mater. Eng.*, **2017**, **46**(8):2065-2069

[17]TAN De-Xin(谭德新), WANG Yan-Li(王艳丽), GAN Ying (甘影), et al. *Chinese J. Inorg. Chem.*(无机化学学报), **2016**, **32**(3):475-482

[18]Pan H B, Wai C M. *New J. Chem.*, **2011**,**35**(8):1649-1660

[19]Yuan Q, Zhuang J, Wang X. *Chem. Commun.*, **2009**,**43**:6613-6615

[20]Kim K, Kim K L, Shin K S. *J. Phys. Chem. C*, **2011**,**115**(30):14844-14851

[21]Chen J Y, Wiley B J M, Mclellan J, et al. *Nano Lett.*, 2005, **5**(10):2058-2062

[22]Qiu Y, Xin L, Chadderdon D J, et al. *Green Chem.*, **2014**, **16**(3):1305-1315

[23]Kibsgaard J, Gorlin Y, Chen Z B, et al. *J. Am. Chem. Soc.*, **2012**,**134**(18):7758-7765

[24]Zhu C Z, Guo S J, Dong S J. *Chem. Eur. J.*, **2013**,**19**(3):1104-1111

[25]Liang Z X, Zhao T S, Xu J B, et al. *Electrochim. Acta*, **2009**,**54**(8):2203-2208

[26]Peng C, Hu Y, Liu M, et al. *J. Power Sources*, **2015**,**278**:69-75

[27]Sun Z P, Zhang X G, Liang Y Y, et al. *Electrochem. Commun.*, **2009**,**11**(3):557-561

[28]An C L, Kuang Y F, Fu C P, et al. *Electrochem. Commun.*, **2011**,**13**(12):1413-1416

[29]Hu G Z, Nitze F, Barzegar H R, et al. *J. Power Sources*, **2012**,**209**:236-242